scientific reports

Check for updates

OPEN

Enhanced oral delivery and bioactivity of EGCG via DNA nanocarriers

Daniela Alvim Chrisostomo[1], Dimitra Athanasiadou[1], Denise Eymael[1], Tulika Sarma[2], Cristiane Duque[1,3], Anuradha Prakki[1]✉ & Karina M. M. Carneiro[1,4]✉

Herein we describe epigallocatechin gallate (EGCG), a bioactive green tea extract, loading onto DNA nanostructures [DNA tetrahedron (TDNs) and DNA hydrogel (DH)] for improved bioavailability and biological activity. TDN-EGCG incorporation was confirmed by circular dichroism (CD), UV spectroscopy and gel electrophoresis (PAGE). Degradation kinetics of TDN and DH, with and without EGCG were measured for up to 14 days and quantified by PAGE. TDN-EGCG showed slower degradation than TDN in human saliva, while both nanostructures remained stable in artificial saliva for up to 48 h. DH-EGCG showed improved stability compared to the hydrogel alone. Human gingival fibroblasts exposed to neat-EGCG, TDN-EGCG, TDN, or buffer were analyzed for cell viability, total protein quantification, and cytokines expression levels. Cell viability and total protein levels did not differ from controls. The inhibitory effect of TDN and TDN-EGCG on *Streptococcus mutans* biofilms was also investigated. TDN-EGCG reduced IL-6, IL-8, and MCP-1 at 6 h and IL-6 and MCP-1 at 24 h timepoints, and inhibited *S. mutans* biofilm formation after 6 h. Statistical analyses were performed using one-way ANOVA and Tukey's post-hoc test ($\alpha = 0.05$). These findings highlight TDNs as promising EGCG carriers and support DH-EGCG as a complementary delivery system.

Keywords EGCG, Tetrahedral DNA nanostructures, DNA hydrogels, Cytotoxicity, Biofilms, Cytokines

Epigallocatechin gallate (EGCG), the most abundant and bioactive polyphenol in green tea, is known for its cytocompatibility and therapeutic properties, including antimicrobial, anti-inflammatory, antioxidant, and antiproteolytic effects[1,2]. These effects are maintained even when EGCG is covalently bonded to polymers or incorporated into dental materials[1]. However, its clinical potential is limited by poor stability in neutral and alkaline environments, leading to degradation and reduced bioactivity[3]. Encapsulation into nanoscale carriers has been proposed to enhance EGCG's stability and therapeutic performance[4,5]. However, there is limited research on the loading of EGCG into nanostructures and delivery to date.

Chemically, EGCG contains four rings (A, B, C, and D), including three aromatic rings that can interact with DNA duplexes via terminal base-pair stacking, intercalation, or groove binding[6]. Based on visual inspection of representative structures obtained from clustering analysis, Galindo-Murillo R. and Cheatham T.E. (2018)[6] suggested that ring A facilitates conformational rearrangement of rings B and D, thereby enhancing non-bonded interactions with DNA and contributing to stabilization of the overall complex. DNA nanotechnology is a field where DNA duplexes are used for the construction of biocompatible and stimuli-responsive materials based on sequence design[7]. These nanostructures have been shown to improve drug stability and transport, enhance permeation to the target site, and reduce toxicity and side effects, thereby increasing therapeutic efficacy[8]. DNA nanostructures have been shown to enhance drug solubility, systemic circulation, cellular penetration, and internalization[8].

Tetrahedral DNA nanostructures (TDNs) in particular, assembled from four single DNA strands (Fig. 1a), have shown great potential for drug delivery. TDNs are flexible, high-capacity carriers capable of penetrating cells without the need for transfection agents, an especially attractive feature for drug delivery platforms[9–11]. Recently, TDNs loaded with EGCG were successfully used for inner ear therapies[12]. In addition to TDNs, DNA hydrogels (DH), three-dimensional DNA networks embibed with water[7], have recently gained attention as drug

[1]Faculty of Dentistry, University of Toronto, 124 Edward Street, Room 547, Toronto, ON M5G1G6, Canada. [2]Science Department, Triton College, River Grove, IL, USA. [3]Faculty of Dental Medicine, Centre for Interdisciplinary Research in Health, Universidade Católica Portuguesa-UCP, Viseu, Portugal. [4]Tier 2 Canada Research Chair in DNA-Based Biomaterials, Faculty of Dentistry and Institute of Biomedical Engineering, University of Toronto, 124 Edward Street, Room 493, Toronto, ON M5G1G6, Canada. ✉email: a.prakki@dentistry.utoronto.ca; karina.carneiro@utoronto.ca

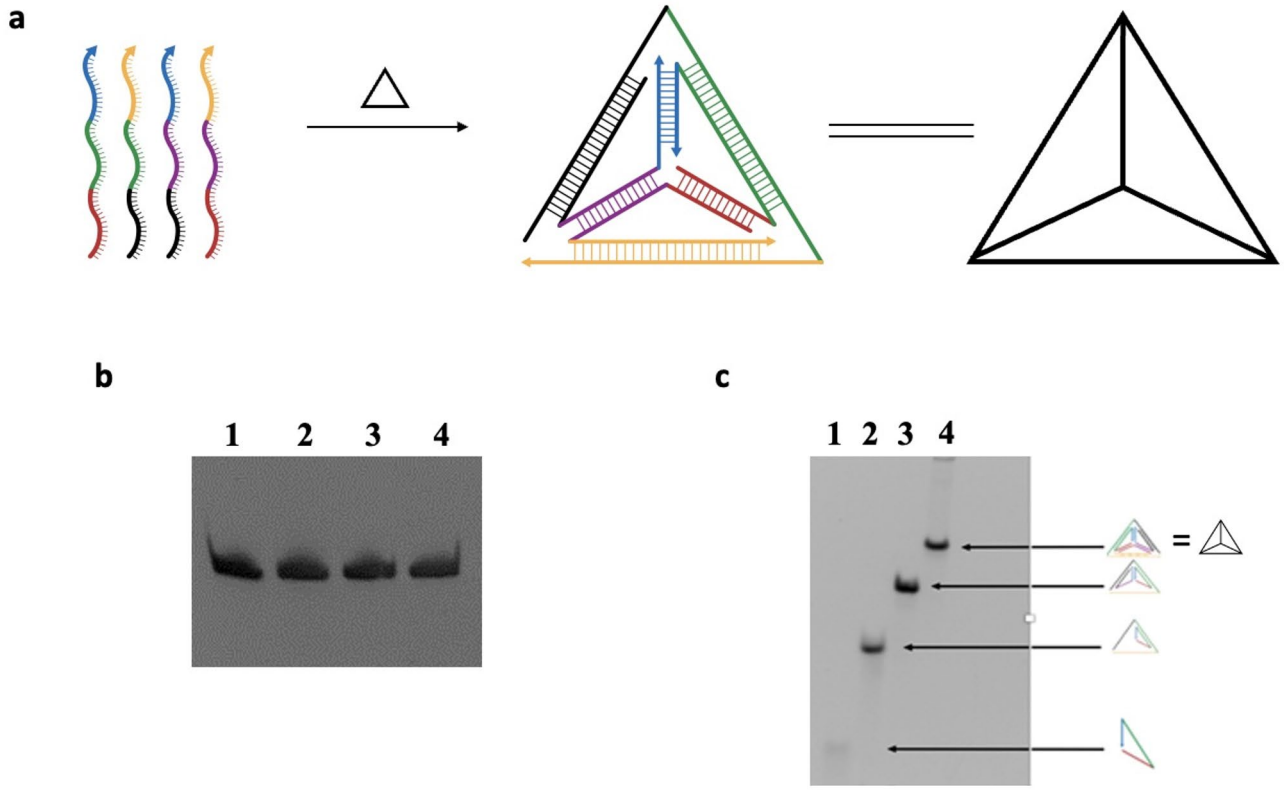

Fig. 1. TDN self-assembly. (**a**) Schematic representation of four DNA strands assembly into a tetrahedral shape based on sequence design; (**b**) 15% denaturing PAGE of strands 1–4 and (**c**) 8% native PAGE of self-assembly of strands 1–4 into a TDN.

and cell carriers for therapeutic applications, including bone repair[7,13], osteoarthritis[14] and diabetic foot ulcer treatments[15]. Therefore, the EGCG-loaded hydrogels developed herein could show promise in both regenerative medicine and dentistry.

Herein we aimed to gain a deeper understanding of the loading of EGCG onto DNA nanostructures (i.e., TDN and DNA hydrogel), and to characterize their assembly, degradation kinetics, cytocompatibility, cytokine expression and antimicrobial effects. We *hypothesize* that EGCG can be loaded onto TDN and DNA hydrogel without affecting their structure, while enhancing EGCG's biological activity. Our long-term goal is to develop EGCG-loaded DNA nanostructures as novel drug delivery systems for oral applications.

Results

Characterization of TDN and TDN-EGCG

DNA strands were purchased from IDT DNA and used without further purification. The purity of DNA strands was confirmed by 15% denaturing PAGE showing strands as single bands; and the DNA strand assembly into a tetrahedron was verified by 8% native PAGE (Fig. 1).

Figure 2 showsa schematic and photo representations of TDN loaded with EGCG and its confirmation through the 8% native PAGE.

The conformational polymorphism of the TDN nanostructure was evaluated by performing circular dichroism (**CD**) spectroscopy of the TDN with and without EGCG. Our results confirmed the intact assembly of modified tetrahedron after EGCG incorporation. CD showed that the intensity of TDN structure changed after EGCG intercalation, reflecting conformational shifts in the DNA helices consistent with DNA duplex intercalation. For TDN alone, a strong negative peak at 227–261 nm and a strong positive one at 261–296 nm were noted. For TDN-EGCG, less pronounced peaks were also observed in the same regions. The entrapment concentration of EGCG inside the TDN after washing was calculated based on the standard curve obtained using UV-vis absorption measurements at 274 nm. The average concentration of the loaded EGCG inside the TDN was calculated to be 134.1 μM (Fig. 3).

TDN and TDN-EGCG were stable in artificial saliva for up to 48 h. In addition, TDN-EGCG exhibited a slightly superior stability compared to TDN when both were incubated in human saliva (Fig. 4).

The DH-EGCG constructs developed in this study (Fig. 5a), prepared via gradual incorporation of EGCG, demonstrated good stability in 10% fetal bovine serum (FBS) for up to 14 days (Fig. 5b).

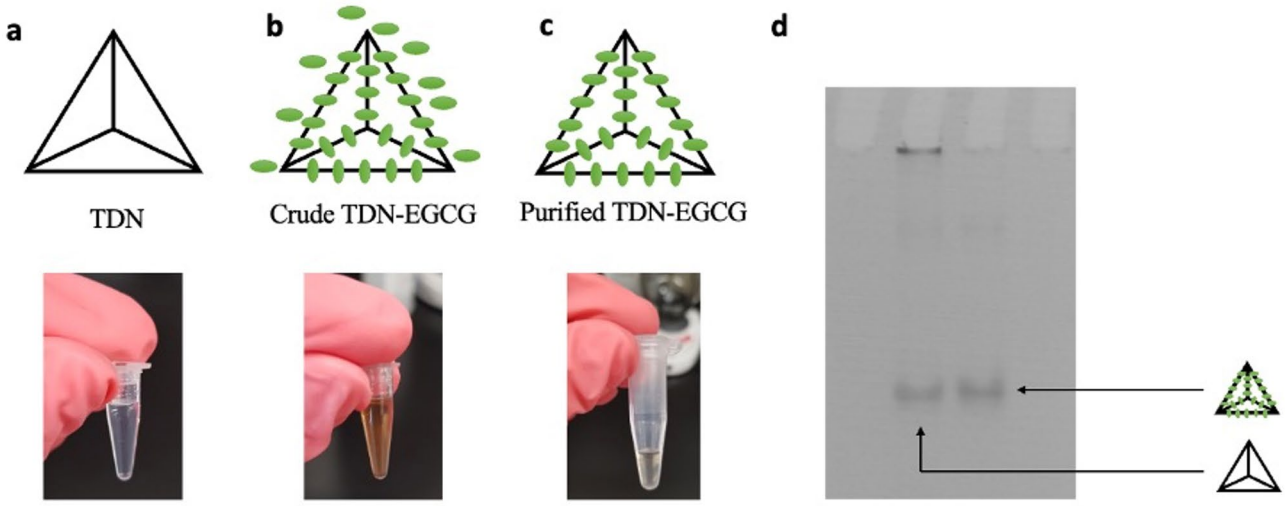

Fig. 2. Loading EGCG onto TDN. Schematic representation (top) and pictures (bottom) of formulations containing: (**a**) TDN alone; (**b**) TDN-EGCG crude mixture before purification, (**c**) purified TDN-EGCG after removal of unbound EGCG and (**d**) 8% native PAGE of purified TDN-EGCG solution confirming successful loading and structural integrity.

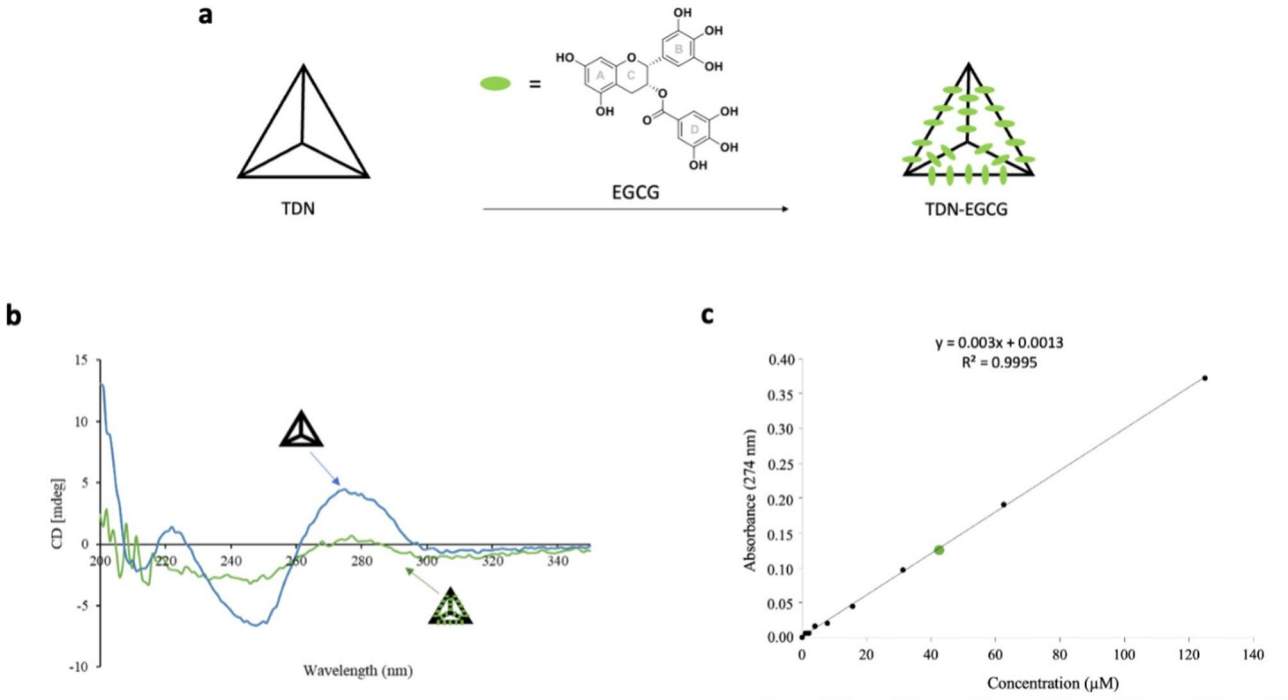

Fig. 3. EGCG incorporation within TDN. (**a**) Schematic of epigallocatechin gallate (EGCG) loading onto a tetrahedral DNA nanostructure (TDN). (**b**) Circular dichroism (CD) spectra of TDN (blue) and TDN-EGCG (green), indicating structural changes consistent with intercalation between base pairs upon EGCG incorporation. (**c**) Quantification of the amount of EGCG loaded onto TDN (green dot) measured by UV-vis spectroscopy (λ = 274 nm), after purification.

Biological characterization of TDN and TDN-EGCG

The effect of TDN, TDN-EGCG and neat-EGCG on fibroblasts viability following 6 h and 24 h of treatments are shown in Figure S1. Cell viability was higher than 100% for both TDN and TDN-EGCG at both time points, indicating the cytocompatibility of the formulations. In contrast, neat-EGCG reduced cell viability compared to the other groups, particularly at 24 h ($p < 0.05$). Regarding protein concentration, no statistically significant differences were observed when TDN or TDN-EGCG were compared with the controls and neat-EGCG after

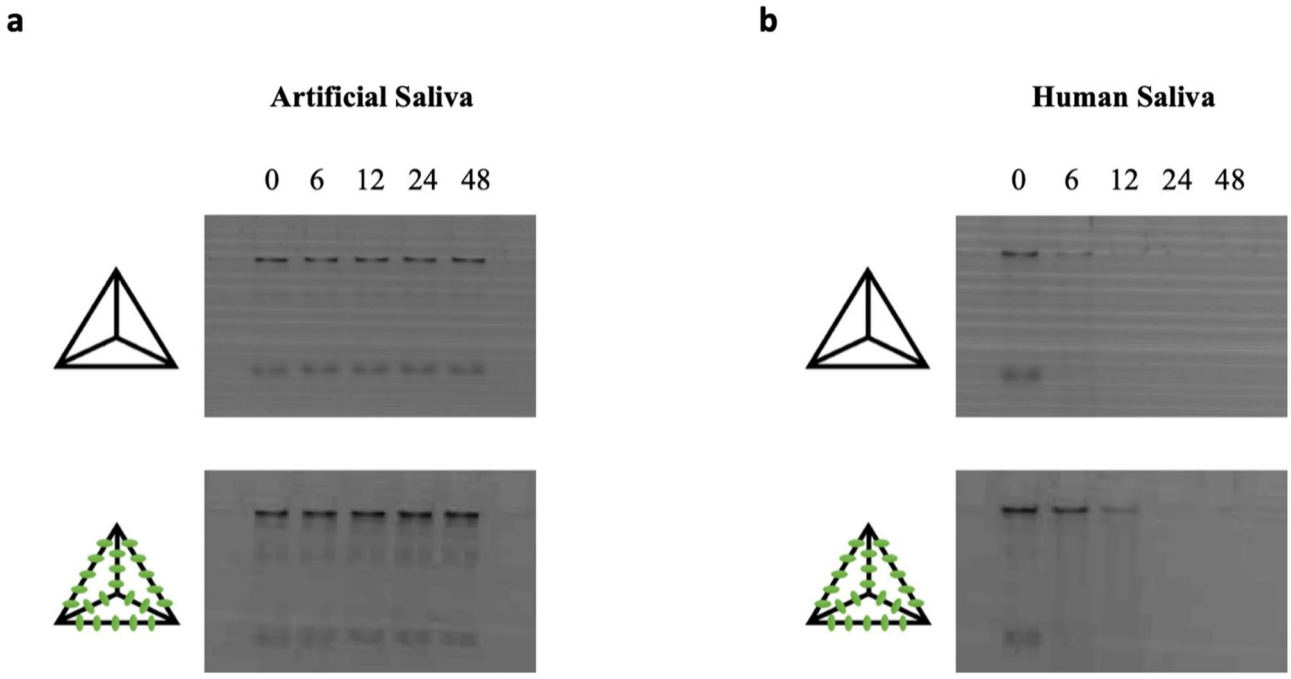

Fig. 4. Stability of TDN and TDN-EGCG in artificial and human saliva. 8% native PAGE characterization of TDN (top) and TDN-EGCG (bottom) degradation in: (**a**) artificial saliva; and (**b**) human saliva.

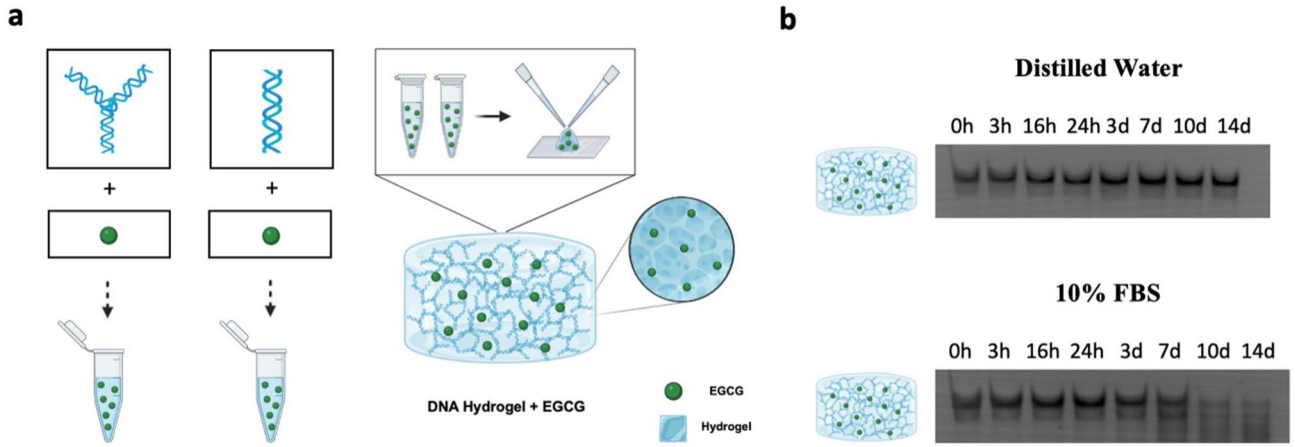

Fig. 5. EGCG incorporation within DNA hydrogel (DH). (**a**) Schematic of EGCG loading onto DNA hydrogel. (**b**) 15% denaturing PAGE characterization of DH-EGCG degradation in distilled water (top) and in 10% FBS (bottom), demonstrating the stability of the formulation in different conditions.

6–24 h of treatment ($p > 0.05$), showing that total protein content was not affected by the formulations (Figure S2). At 6 h, TDN-EGCG reduced IL-6, IL-8, and MCP-1 levels compared to TDN and buffer controls ($p < 0.05$), and at 24 h, IL-6 and MCP-1 levels were lower for TDN-EGCG than those detected in culture medium ($p < 0.05$) (Figure S3). Levels of IL-6, IL-8, and MCP-1 were drastically reduced at both time points in cells treated with neat-EGCG, except for IL-6 at 24 h. Considering the antibiofilm effect, TDN-EGCG inhibited *S. mutans* biofilms after 6 h of application ($p < 0.05$) with no difference detected in biofilms after 24 h of treatment ($p > 0.05$) (Figure S4).

Discussion

TDN, a three-dimensional tetrahedral frame structure formed by hybridization of four DNA strands[16], has been proposed as a promising drug carrier due to its high stability, biocompatibility, functional modification sites, suitability for different drugs and excellent cellular uptake rates[11,17]. TDN has been previously investigated as a drug carrier for cancer therapy[18], osteoarthritis[17] and hearing loss[12], but not for oral applications. As

hypothesized, EGCG was successfully incorporated into TDN and hydrogel, and our results indicate that this formulation has the potential to enhance its bioavailability and biological activity. Native PAGE analysis demonstrated that EGCG loading did not affect the hybridization of DNA strands into the TDN, in agreement with a previous study[12].

In circular dichroism results, a notable decrease in the TDN absorption peak upon the addition of EGCG indicated the intercalation of EGCG into double-stranded DNA (dsDNA) of TDNs. Similar findings have been reported regarding the interaction of flavonoids and quinones with DNA duplexes[12,19], suggesting the potential for incorporating compounds with analogous structures into DNA nanostructures. Computational studies demonstrated that EGCG can interact with DNA through a combination of intercalation and groove binding modes, stabilized by hydrogen bonding and stacking interactions with nucleobases[6]. These findings support the notion that EGCG–DNA binding is multifactorial. Collectively, these interactions may play a key role in both the binding affinity of EGCG to DNA nanostructures and the enhanced structural stability observed in the present system. The entrapment concentration of EGCG was calculated based on the standard curve obtained using UV-vis absorption measurements at 274 nm. The averaged concentration of the intercalated EGCG was 134.1 μM, corresponding to ~ 43 EGCG molecules per TDN.

TDN-EGCG exhibited superior stability compared to TDN when both were incubated in human saliva. The slower degradation rates of TDN-EGCG indicate that the incorporation of EGCG into TDN may enhance its resistance to degradation in biological environments. It is known that the strong binding affinity of EGCG to DNA can suppress the activity of several enzymes, such as nucleases, collagenases and hyaluronidases, by blocking their active sites protecting DNA from in vivo serum protease-mediated degradation[20]. Although artificial saliva was used to assess the stability of the nanocarriers, as it provides controlled and reproducible conditions, human saliva represents the most realistic environment for oral applications due to its complex composition and variability. In the present study, both TDN and TDN-EGCG exhibited stability in artificial saliva for up to 48 h. However, in human saliva, stability was observed for up to 12 h, which is still a promising indicator of resistance under natural oral conditions. These results suggest that the nanocarriers can withstand adverse conditions in the oral cavity for a significant period. The maintenance of nanostructure integrity in artificial and human saliva highlights the potential of TDNs for controlled-release formulations and other oral delivery systems.

Biocompatibility is a crucial property for any compound recommended for oral applications. In the present study, both TDN and TDN-EGCG did not affect the cell viability of fibroblasts exposed to those formulations after 6 and 24 h, with viability higher than 100% at both time points. In previous studies, TDNs exhibited cytocompatibility and stimulated cell metabolism in various cell lines, such as mouse L929 fibroblasts, human corneal epithelial cells, and chondrocytes, among others[21,22]. EGCG has also been previously evaluated in fibroblasts and shown cytocompatibility at concentrations lower than 1 mg/mL[2,23–25], much higher than that evaluated in the present study (~ 130 μM, 60 μg/mL).

Considering the levels of cytokines, our results indicate that TDN-EGCG was able to release EGCG and reduce the presence of pro-inflammatory markers. It is relevant to mention that cells were not previously exposed to any inflammatory molecules, such as lipopolysaccharides that can trigger the production of pro-inflammatory cytokines and chemokines, reactive oxygen-species or nitric oxide[26]. Further, while TDN was considered cytocompatible, it stimulated minimal inflammatory response that was attenuated by the presence of EGCG. In this study, neat-EGCG (250 μM) markedly reduced or even suppressed cytokine production at most of the time points evaluated, suggesting that high concentrations of EGCG could cause global transcriptional inhibition, thereby impairing the immune response. This observation is consistent with previous reports indicating that higher levels (> 150 μM) of EGCG are associated with cytotoxicity and broad inhibition of cellular transcription, raising concerns regarding its physiological relevance and clinical translatability[27–29]. In contrast, when delivered via TDN, the effective EGCG concentration was approximately 130 μM, resulting in a more moderate reduction in cytokine production, suggesting a more controlled immunomodulatory effect.

In another study, contrary to our findings, however, in the presence of LPS, TDN reduced the expression of IL-1β (interleukin-1β), IL-6, and TNF-α (tumor necrosis factor-α) in LPS-induced RAW264.7 macrophage cells by inhibiting MAPK phosphorylation[30]. In a previous study, human mast cells (HMC-1) were stimulated with phorbol 12-myristate 13-acetate (PMA) plus calcium ionophore (A23187) and treated with EGCG at 100 μM. EGCG inhibited TNF-α, IL-6 and IL-8 expression and production as analyzed by ELISA and Western-blot. The authors suggested that EGCG can be helpful in regulating inflammatory response[31]. In a tri-dimensional co-culture model of fibroblast and epithelial cells, EGCG reduced the secretion of various cytokines, including IL-6, IL-8, and had no effect on MCP-1 secretion[32]. EGCG was the most effective catechin at inhibiting IL-6 and IL-8 production by 59% and 57% in rheumatoid arthritis synovial fibroblasts, respectively[33].

Considering the antibiofilm effect, TDN-EGCG inhibited *S. mutans* biofilm growth after 6 h of application but had no significant effect after 24 h. The greater efficacy at 6 h may be attributed to the stronger initial action of TDN-EGCG, when the biofilm is in an early, more susceptible stage, characterized by a thinner, less extensive extracellular matrix and lower bacterial density[34]. Notably, neat-EGCG, although at a higher concentration (250 μM) than that released from TDN EGCG (around 130 μM), did not reduce *S. mutans* counts in biofilms compared to the control. Previous studies have reported that EGCG inhibits *S. mutans* biofilms at much higher concentrations (above 500 μg/mL, 1 M)[35,36]. Additionally, DNA-based nanomaterials, such as TDN, have demonstrated enhanced biofilm penetration and retention, enabling a sustained local release of antimicrobial agents and promoting their accumulation within the biofilm over time[37]. In a 24 h in vitro model of multidrug-resistant *Acinetobacter baumannii* biofilms, polymyxin B-loaded TDN increased biofilm permeability by approximately 6-fold relative to free polymyxin B, resulting in enhanced biofilm disruption and a significant reduction in bacterial density after 3 h of treatment[38].

Previous studies have shown that topical EGCG treatment impaired *S. mutans* biofilm initial growth and maturation, reducing the synthesis of biofilm matrix components and altering the biofilm matrix structure, organization, and distribution[23,25,39]. A molecular docking study showed that EGCG potentially binds to the *S. mutans* glucan sucrase and inhibits its enzymatic activity, attenuating biofilm formation potential of *S. mutans* on the tooth surfaces[40]. It is important to point out that the EGCG concentrations used in those studies were between 0.125 and 4 mg/mL, much higher than the concentration of EGCG release from TDN-EGCG (~ 130 µM, 60 µg/mL). This is the first study evaluating the inhibitory effect of TDN-EGCG on oral biofilms. The effect of EGCG-loaded nanoparticles against *S. mutans* biofilm was reported in previous studies[4,41]. In chitosan nanoparticles, EGCG had no effect on microbial viability; however, the EGCG-nanoformulations disassembled the biofilm matrix[4]. EGCG-encapsulated nanohydroxyapatite/mesoporous silica nanoparticles showed lower cellular metabolic activity and fewer bacterial colonies in *S. mutans* biofilms compared to the control group[41].

Lastly, we performed a pilot experiment with DNA hydrogels as EGCG carriers. DHs offer several advantages, including tunable mechanical properties[42,43]. Various strategies have been developed to synthesize DHs for biomedical applications, such as biosensing, drug delivery, tissue engineering, and cell culture[44]. In this context, the DH-EGCG constructs developed in this study demonstrated good stability in 10% FBS for up to 14 days. While we did not experimentally evaluate the DH without EGCG in the current study, our results suggest slower degradation (~ 14 d) compared to previously published data by our lab[7] of DH only (~ 7 d). These findings highlight the potential of EGCG incorporation to enhance the structural stability of DNA hydrogels under physiological conditions.

Some limitations of the study should be addressed. This study evaluated a limited number of cytokines, and anti-inflammatory cytokines could be included in future studies to analyze if TDN-EGCG affects other inflammatory markers. Other microorganisms such as *Lactobacillus*, *Actinomyces* and *Candida albicans* should also be tested in subsequent studies. Moreover, future investigations involving TDN-EGCG and DH-EGCG, are being planned to evaluate their antimicrobial activity, cytocompatibility, and efficacy.

In summary, TDN is a promising EGCG delivery carrier due to its stability in artificial saliva, low degradation, and cytocompatibility. TDN also promoted efficient in vitro release of EGCG, thereby contributing to reduced cytokine expression and bacterial biofilm formation. DNA hydrogels loaded with EGCG showed the same slower degradation pattern as TDN-EGCG, highlighting its potential as a complementary drug delivery system.

Materials and methods

TDN and DH assembly and EGCG incorporation

TDN (1 µM) was assembled as previously described[45]. EGCG was incorporated by slowly adding 20 µL of 10 mM EGCG on a shaker at room temperature. Excess EGCG was removed using a Sephadex G-25 column. Final [EGCG] was determined by UV-vis measurements at 274 nm using a Cytation 3 Plate Reader Model CYT3MF (BioTek, Winooski, VT, USA). Proper assembly and EGCG incorporation were determined by circular dichroism (CD) and polyacrylamide gel electrophoresis (PAGE). CD spectra were acquired at room temperature using a J-1500 Spectrophotometer (Jasco, Tokyo, Japan). TDN-EGCG interaction experiments were recorded in the range 350 –200 nm, averaged 3 scans and 1 nm bandwidth. Denaturing PAGE was run at 15 mA and 300 V for 1.5 h, after which the gel was stained with GelGreen® (Biotium). Gel imaging was performed using a Gene Genius Bioimaging System (Syngene). Quantification of the gel panels was performed using ImageJ software (version 2.14.0/1.54f). DH was assembled as previously described[7]. EGCG was incorporated by slowly adding 50 µL of 1 mM of EGCG solution. Successful assembly was characterized by PAGE.

Human saliva collection and purification

This study was approved by the University of Toronto Research Ethics Board (REB) under Protocol #00048090. All participants provided verbal and written informed consent prior to sample collection. All methods were carried out in accordance with relevant guidelines and regulations. We recruited 21 healthy participants from the University of Toronto Faculty of Dentistry (124 Edward Street, Toronto): 9 males (26–35 years) and 12 females (23–36 years). The exclusion criteria included intake of any drugs/medicines, existence of any oral disease, autoimmune, infectious, musculoskeletal or malignant disease, and recent operation or trauma. Participants also had to be free of fever and/or cold, non-smokers and had good oral hygiene. Participants were instructed to not have brushed teeth for at least two hours before collection, and to remain at least one hour without consuming food and drinks. Unstimulated saliva was collected for 15 min from each volunteer in Falcon tubes, for a total volume of approximately 7.5 mL. Saliva samples from all 21 volunteers were then combined and frozen in 15 mL tubes. While pooling may limit assessment of individual differences, it is suitable for evaluating biological trends for this in vitro study. Pooling ensures that the sample represents an average biological response across all volunteers, and therefore reducing individual variability. The 15-minute collection period follows widely used protocols for unstimulated saliva, ensuring sufficient sample volume and stable salivary flow. When the saliva was needed for an experiment, it was thawed to room temperature, vortexed, and then centrifuged at 10,000 g for 10 min to remove all debris. The supernatant from each sample was collected and used for experiments. This protocol has been previously described in the literature[46–50].

Degradation kinetics measurements

TDN and DH with and without EGCG were incubated at 37° C for up to 14 days in water (control), 10% fetal bovine serum (FBS), human saliva or artificial saliva[51]. Samples were placed in -20°C at specific timepoints until PAGE characterization. For the TDN with and without EGCG, the PAGE was run as previously described. In the case of DH with and without EGCG, native PAGE was run at 15 mA and 80 V for 16 h.

Cell viability, total protein quantification and cytokine expression

Human gingival fibroblasts (early-passage cells freshly thawed from liquid nitrogen) were maintained in Dulbecco's Modified Eagle's medium (DMEM; with high glucose, L-glutamine, and sodium pyruvate) supplemented with 10% fetal bovine serum (Gibco, Grand Island, NY, USA), with 100 IU/mL of penicillin, 100 mg/mL of streptomycin and 0.25 mg/mL of fungizone (Gibco). Cells were subcultured every 48 h and allowed to grow in a humidified incubator at 37°C with 5% CO_2 (Isotemp; Fisher Scientific, Pittsburgh, PA, USA). After 48 h of growth in DMEM, fibroblasts were seeded in DMEM in a 96-well plate at 2 × 105 cells/well and incubated for 24 h. Then, the cells (n = 9) were exposed to the formulations TDN, TDN-EGCG, neat-EGCG (250 µM) or buffer solution (negative control) for 6 h and 24 h at 37°C. Supernatants were collected for cytokine analysis using the Bio-Plex Pro™ Human Cytokine 27-plex Assay (Bio-Rad Laboratories Inc., Hercules, CA, USA). Cells were stained with Alamar blue assay (Thermo-Fisher Scientific) and after 3 h, supernatants were read in a spectrometer at 550 and 600 nm (Cytation 3, Bio-Tek, Bio-Tek, Winooski, VT). The percentage of cell viability was determined relative to the control (DMEM culture medium, 100% cell viability)[52]. After scraping, cell lysis was conducted using 1x RIPA Buffer (Cell Signaling Technologies, MA, USA), centrifugation at 13,000 rpm for 10 min and supernatants were analyzed by Pierce Bicinchoninic acid (BCA) assay (Thermo Scientific #23225, Waltham, MA) and read in a spectrophotometer at 562 nm for total protein quantification[24].

Antimicrobial activity

The assays were conducted as previously described[23]. Colonies of *S. mutans* (ATCC 25125) previously grown in Mitis Agar Salivarius (Difco Laboratories) containing 0.2 U/mL bacitracin were inoculated in Brain Heart Infusion (BHI) broth and incubated for 24 h at 37°C in 5% CO_2 atmosphere. The resultant cultures were adjusted to the optical density 0.5 (Absorbance 550 nm), diluted 1000x and centrifuged and inoculated in BHI broth supplemented with 0.5% sucrose (approximately 1–5 × 10^6 CFU/mL). For biofilm formation, a pretreatment with 200 µL/well of artificial saliva (composition: 800 mL of deionized water, 1.6 g of yeast extract, 4 g of peptone, 0.28 g of NaCl, 1.6 g of glucose or 3.2 g of sucrose, 0.16 g of $CaCl_2$, 0.16 g of KCl and 0.8 g of mucin) was applied in U-shaped bottom 96-well microplates for 4 h at 37°C. Afterwards, saliva was aspirated and 200 µL of *S. mutans* culture was inoculated in each well and incubated for 24 h. After that, 100 µL of the compounds (TDN, TDN-EGCG, neat-EGCG (250 µM) and buffer as negative control) or culture media (positive control) were applied to biofilms for 6 h and 24 h. Then, the treatments were removed and 100 µL of 0.9% NaCl solution were added to each well for further dilution, plated in BHI agar, and incubated for 48 h. After this period, the colony forming units/mL (CFU/mL) were determined and values transformed in $\log_{10}$ (CFU/mL).

Statistical analysis

SPSS 19.0 software (SPSS Inc., Chicago, IL, USA) was used. Data were expressed in means ± standard deviations unless otherwise stated. Normality and homogeneity of variance were assessed using Shapiro–Wilk and Levene tests, respectively. Data were then analyzed using one-way ANOVA followed by Tukey post-hoc tests ($\alpha = 0.05$).

Data availability

The datasets produced and evaluated in the present work are available from the corresponding author upon reasonable request.

Received: 14 February 2026; Accepted: 30 April 2026
Published online: 08 May 2026

References

1. Prakki, A. et al. Functionalized epigallocatechin gallate copolymer inhibits dentin matrix degradation: Mechanical, solubilized telopeptide and proteomic assays. *Dent. Mater.* **34** (11), 1625–1633 (2018).
2. Chrisostomo, D. A. et al. Antibiofilm properties, cytotoxicity, and effect on protease activity of antibiotics and EGCG-based medications for endodontic purposes. *J. Dent.* **156**, 105660 (2025).
3. Song, H. et al. Antioxidant activity, storage stability and in vitro release of epigallocatechin-3-gallate (EGCG) encapsulated in hordein nanoparticles. *Food Chem.* **388**, 132903 (2022).
4. Aragão, M. G. B., Tedesco, A. C., Borges, H. S., Aires, C. P. & Corona, S. A. M. Chitosan nanoparticles loaded with epigallocatechin-3-gallate: synthesis, characterization, and effects against Streptococcus mutans biofilm. *Nat. Prod. Res.* **39** (9), 2550–2557 (2025).
5. Peng, X., McClements, D. J., Liu, X. & Liu, F. EGCG-based nanoparticles: synthesis, properties, and applications. *Crit. Rev. Food Sci. Nutr.* **65** (12), 2177–2198 (2025).
6. Galindo-Murillo, R. & Cheatham, T. E. Computational DNA binding studies of (-)-epigallocatechin-3-gallate. *J. Biomol. Struct. Dyn.* **36** (13), 3311–3323 (2018).
7. Athanasiadou, D. et al. DNA hydrogels for bone regeneration. *Proc. Natl. Acad. Sci. U S A.* **120** (17), e2220565120 (2023).
8. Kumar, M., Jha, A. & Mishra, B. DNA-Based Nanostructured Platforms as Drug Delivery Systems. *Chem. Bio Eng.* **1** (3), 179–198 (2024).
9. Seitz, I. et al. Prospective Cancer Therapies Using Stimuli-Responsive DNA Nanostructures. *Macromol. Biosci.* **21** (12), e2100272 (2021).
10. Wang, T., Liu, Y., Wu, Q., Lou, B. & Liu, Z. DNA nanostructures for stimuli-responsive drug delivery. *Smart Mater. Med.* **3**, 66–84 (2022).
11. Zhang, T. et al. DNA nanomaterials targeting toll-like receptor 4 prevent bisphosphonate-related osteonecrosis of the jaw via regulating mitochondrial homeostasis in macrophages. *Adv. Funct. Mater.* **33**. (2023).
12. Chen, Y. et al. Epigallocatechin gallate-loaded tetrahedral DNA nanostructures as a novel inner ear drug delivery system. *Nanoscale* **14** (22), 8000–8011 (2022).
13. Meshry, N. & Carneiro, K. M. M. DNA as a promising biomaterial for bone regeneration and potential mechanisms of action. *Acta Biomater.* **197**, 68–86 (2025).
14. Yan, X. et al. Anti-Friction MSCs Delivery System Improves the Therapy for Severe Osteoarthritis. *Adv. Mater.* **33** (52), e2104758 (2021).

15. Se, A. M., Li, L. & Yu, M. Poloxamer-based hydrogel with EGCG and rhEGF for diabetic foot ulcer treatment. *J. Mater. Sci. Mater. Med.* **36** (1), 65 (2025).
16. Zhang, T., Tian, T. & Lin, Y. Functionalizing Framework Nucleic-Acid-Based Nanostructures for Biomedical Application. *Adv. Mater.* **34** (46), e2107820 (2022).
17. Sirong, S. et al. Effects of tetrahedral framework nucleic acid/wogonin complexes on osteoarthritis. *Bone Res.* **8**, 6 (2020).
18. Yan, J. et al. Tetrahedral DNA nanostructures for effective treatment of cancer: advances and prospects. *J. Nanobiotechnol.* **19** (1), 412 (2021).
19. Sun, Y. et al. Study on the interaction mechanism between DNA and the main active components in Scutellaria baicalensis Georgi. *Sens. Actuators B Chem.* **129** (2), 799–810 (2008).
20. Shui, M. et al. Engineering polyphenol-based carriers for nucleic acid delivery. *Theranostics* **13** (10), 3204–3223 (2023).
21. Liu, N. et al. Tetrahedral Framework Nucleic Acids Promote Corneal Epithelial Wound Healing in Vitro and in Vivo. *Small* **15** (31), e1901907 (2019).
22. Shao, X. et al. Tetrahedral DNA Nanostructure: A Potential Promoter for Cartilage Tissue Regeneration via Regulating Chondrocyte Phenotype and Proliferation. *Small* ;**13**(12). (2017).
23. Caiaffa, K. S. et al. Cytocompatibility and Synergy of EGCG and Cationic Peptides Against Bacteria Related to Endodontic Infections, in Planktonic and Biofilm Conditions. *Probiotics Antimicrob. Proteins.* **13** (6), 1808–1819 (2021).
24. Stavroullakis, A. T., Goncalves, L. L., Levesque, C. M., Kishen, A. & Prakki, A. Interaction of epigallocatechin-gallate and chlorhexidine with Streptococcus mutans stimulated odontoblast-like cells: Cytotoxicity, Interleukin-1β and co-species proteomic analyses. *Arch. Oral Biol.* **131**, 105268 (2021).
25. Duque, C. et al. Synergistic antimicrobial potential of EGCG and fosfomycin against biofilms associated with endodontic infections. *J. Appl. Oral Sci.* **31**, e20220282 (2023).
26. Page, M. J., Kell, D. B. & Pretorius, E. The Role of Lipopolysaccharide-Induced Cell Signalling in Chronic Inflammation. *Chronic Stress (Thousand Oaks).* **6**, 24705470221076390 (2022).
27. Sehm, J., Polster, J. & Pfaffl, M. W. Effects of varied EGCG and (+)-catechin concentrations on proinflammatory cytokines mRNA expression in cona-stimulated primary white blood cell cultures. *J. Agric. Food Chem.* **53** (17), 6907–6911 (2005).
28. Rasheed, Z. et al. Green tea polyphenol epigallocatechin-3-gallate inhibits advanced glycation end product-induced expression of tumor necrosis factor-alpha and matrix metalloproteinase-13 in human chondrocytes. *Arthritis Res. Ther.* **11** (3), R71 (2009).
29. Payne, A., Taka, E., Adinew, G. M. & Soliman, K. F. A. Molecular Mechanisms of the Anti-Inflammatory Effects of Epigallocatechin 3-Gallate (EGCG) in LPS-Activated BV-2 Microglia Cells. *Brain Sci.* **13** (4), 632 (2023).
30. Zhang, Q. et al. Anti-inflammatory and Antioxidative Effects of Tetrahedral DNA Nanostructures via the Modulation of Macrophage Responses. *ACS Appl. Mater. Interfaces.* **10** (4), 3421–3430 (2018).
31. Shin, H. Y. et al. Epigallocatechin-3-gallate inhibits secretion of TNF-alpha, IL-6 and IL-8 through the attenuation of ERK and NF-kappaB in HMC-1 cells. *Int. Arch. Allergy Immunol.* **142** (4), 335–344 (2007).
32. Lombardo Bedran, T. B., Palomari Spolidorio, D. & Grenier, D. Green tea polyphenol epigallocatechin-3-gallate and cranberry proanthocyanidins act in synergy with cathelicidin (LL-37) to reduce the LPS-induced inflammatory response in a three-dimensional co-culture model of gingival epithelial cells and fibroblasts. *Arch. Oral Biol.* **60** (6), 845–853 (2015).
33. Fechtner, S., Singh, A., Chourasia, M. & Ahmed, S. Molecular insights into the differences in anti-inflammatory activities of green tea catechins on IL-1β signaling in rheumatoid arthritis synovial fibroblasts. *Toxicol. Appl. Pharmacol.* **329**, 112–120 (2017).
34. Almatroudi, A. Biofilm Resilience: Molecular Mechanisms Driving Antibiotic Resistance in Clinical Contexts. *Biology* **14** (2), 165 (2025).
35. Schneider-Rayman, M., Steinberg, D., Sionov, R. V., Friedman, M. & Shalish, M. Effect of epigallocatechin gallate on dental biofilm of Streptococcus mutans: An in vitro study. *BMC Oral Health.* **21** (1), 447 (2021).
36. Wu, C. Y. et al. Inhibitory effects of tea catechin epigallocatechin-3-gallate against biofilms formed from Streptococcus mutans and a probiotic lactobacillus strain. *Arch. Oral Biol.* **94**, 69–77 (2018).
37. Sousa, A. et al. Decoding interactions between biofilms and DNA nanoparticles. *Biofilm* **9**, 100260 (2025).
38. Hu, Y. et al. A novel tetrahedral framework nucleic acid-based antibiotic delivery system: overcoming biofilm barriers to combat chronic infections. *J. Nanobiotechnol.* **23** (1), 465 (2025).
39. Aragão, M. G. B., Aires, C. P., Corona, S. A. M. & He, X. Effects of epigallocatechin gallate on the development of matrix-rich Streptococcus mutans biofilm. *Biofouling* **41** (2), 171–180 (2025).
40. Hairul Islam, M. I. et al. Inhibitory potential of EGCG on Streptococcus mutans biofilm: A new approach to prevent Cariogenesis. *Microb. Pathog.* **143**, 104129 (2020).
41. Yu, J. et al. Development of Epigallocatechin-3-gallate-Encapsulated Nanohydroxyapatite/Mesoporous Silica for Therapeutic Management of Dentin Surface. *ACS Appl. Mater. Interfaces.* **9** (31), 25796–25807 (2017).
42. Oishi, M. & Nakatani, K. Dynamically Programmed Switchable DNA Hydrogels Based on a DNA Circuit Mechanism. *Small* **15** (15), e1900490 (2019).
43. Sun, Y., Li, S., Chen, R., Wu, P. & Liang, J. Ultrasensitive and rapid detection of T-2 toxin using a target-responsive DNA hydrogel. *Sens. Actuators B.* **311**, 127912 (2020).
44. Wu, R. et al. DNA hydrogels and their derivatives in biomedical engineering applications. *J. Nanobiotechnol.* **22** (1), 518 (2024).
45. Zhou, M. et al. Effect of tetrahedral DNA nanostructures on proliferation and osteogenic differentiation of human periodontal ligament stem cells. *Cell. Prolif.* **52** (3), e12566 (2019).
46. Mohamed, R., Campbell, J. L., Cooper-White, J., Dimeski, G. & Punyadeera, C. The impact of saliva collection and processing methods on CRP, IgE, and Myoglobin immunoassays. *Clin. Transl Med.* **1** (1), 19 (2012).
47. PelÁ, V. T., Ventura, T. M. O. & Buzalaf, M. A. R. Optimizing the formation of the acquired enamel pellicle in vitro for proteomic analysis. *J. Appl. Oral Sci.* **28**, e20200189 (2020).
48. Toro-Alzate, M., Cañas-Gutiérrez, A. I. & Parada-Sánchez, M. T. Standardized protocol for unstimulated saliva analysis by ATR-FTIR spectroscopy. *Vib. Spectrosc.* **141**, 103862 (2025).
49. Baek, H. J. et al. Saliva assay: a call for methodological standardization. *J. Periodontal Implant Sci.* **55** (1), 2–17 (2025).
50. Rusthen, S. et al. Dysbiotic salivary microbiota in dry mouth and primary Sjögren's syndrome patients. *PLoS One.* **14** (6), e0218319 (2019).
51. Ablal, M. A. et al. The erosive potential of some alcopops using bovine enamel: an in vitro study. *J. Dent.* **37** (11), 835–839 (2009).
52. Braga, G. P. A. et al. Microbiological properties and cytotoxicity of PNVCL hydrogels containing flavonoids as intracanal medication for endodontic therapy. *J. Funct. Biomater.* **13**(4). (2022).

Acknowledgements

The authors would like to thank Ms. Mercedes Ing for assisting with human saliva collection.

Author contributions

Daniela Alvim Chrisostomo - contributed to the design of the study, data acquisition, analysis and interpretation, drafted the manuscript, and critically revised the manuscript. Dimitra Athanasiadou - contributed to the design of the study, data acquisition, analysis and interpretation, and drafted the manuscript. Denise Eymael

contributed to data acquisition and interpretation and critically revised the manuscript. Tulika Sarma - contributed to the conception and design of the study, and critically revised the manuscript. Cristiane Duque - contributed to the design of the study, data acquisition, analysis and interpretation, and critically revised the manuscript. Anuradha Prakki - contributed to the conception and design of the study, data interpretation, and critically revised the manuscript. Karina M. M. Carneiro - contributed to the conception and design of the study, data interpretation, and critically revised the manuscript. All authors reviewed the manuscript and gave final approval for submission.

Funding

This work was financially supported by Natural Sciences and Engineering Research Council of Canada - Discovery Grants (RGPIN-2018-06489 to AP and RGPIN-2025-04779 to KC) and Colgate-Palmolive Research Agreement (A-2020-0025-OC to AP, KC and TS).

Declarations

Competing interests

The authors declare no competing interests.

Additional information

Supplementary Information The online version contains supplementary material available at https://doi.org/10.1038/s41598-026-51927-8.

Correspondence and requests for materials should be addressed to A.P. or K.M.M.C.

Reprints and permissions information is available at www.nature.com/reprints.

Publisher's note Springer Nature remains neutral with regard to jurisdictional claims in published maps and institutional affiliations.